Theor Chem Account (2009) 122:43–50
DOI 10.1007/s00214-008-0483-y

REGULAR ARTICLE

Ab initio excitation spectrum of the weak H···CO interaction

Mary C. Salazar · Antonio Jose Hernández

Received: 17 July 2008 / Accepted: 18 September 2008 / Published online: 7 October 2008

Abstract The adiabatic interaction energy (IE) in the van der Waals region of the ground $H(^2S)\cdots CO(X^1\Sigma^+)$ and excited $H(^2S)\cdots CO(a^3\Pi)$ electronic states of the $H\cdots CO$ complex is studied in the framework of the supermolecule approach at the RHF-CCSD(T) level of theory. Calculations predict a minimum with $\beta_e = 72°$, $R_e = 6.89a_o$ and $D_e = 34.10\ cm^{-1}$ for the ground X^2A'state. For the excited $^4A'$ state the minimum occurs at $\beta_e = 104°$ and $R_e = 5.90a_o$ with $D_e = 75.42\ cm^{-1}$. The resulting IE of the excited $^4A''$ state reveals two minima separated by a saddle point. The most stable configuration occurs at $\beta_e = 132°$, $R_e = 6.71a_o$ and $D_e = 40.03\ cm^{-1}$. The corresponding vertical excitation energies and corresponding shifts with respect to the isolated CO molecule are calculated as a guideline for future theoretical and experimental work. In order to investigate the use of less demanding correlation methods, test density functional theory calculations using the mPW1PW exchange–correlation functional are also presented for comparison.

Keywords HCO van der Waals molecule · Ab initio calculations · Coupled cluster theory · Vertical excitation spectra · Interaction energy · mPW1PW functional

1 Introduction

The **H···CO** complex, held together by weak intermolecular van der Waals (vdW) dispersion forces, might be considered as an intermediate between the gas and the condensed phase. In particular, this knowledge is essential for the understanding of a variety of biological, chemical and physical phenomena and represents an important step in the chemistry of interstellar molecules [1–3]. Of main importance, vdW molecules are nowadays accessible both to detailed experimental and to reliable quantum mechanical studies. The implementation of high-resolution state selective spectroscopy and controllable sample conditions have contributed to the experimental progress [4–9]. The availability of powerful supercomputers and the development of efficient computational algorithms have made possible the accurate quantum mechanical study of the properties of these vdW molecular systems [10, 11]. Experiments have provided crucial reference for theoretical chemists, and spectral data have played an important part in the development of potential energy surfaces for these complexes. In some cases, however, for which none or insufficient experimental data exist, ab initio calculations remains the only method of choice.

Ab initio, studies of vdW interaction energies have essentially followed two directions. The first regards the interaction between the subsystems as a perturbation, and partitions the energy into terms such as electrostatic, repulsion, polarization, induction and dispersion. The second approach considers the interacting subsystems as a supermolecule [1–3, 10, 11]. Since all the highly effective ab initio methods developed for single-molecule calculations are in principle applicable without change and, it also offers a uniform treatment over the entire range of intermolecular separations, the vast majority of calculations of the interaction energy of vdW complexes are carried out at present using the supermolecule approach. The advent of state-of-the-art computational facilities has made possible to develop many-body methods of electronic structure

M. C. Salazar · A. J. Hernández (✉)
Departamento de Química, Universidad Simón Bolívar,
Apdo. 89000, Caracas 1080A, Venezuela
e-mail: ajher@usb.ve

capable of reliable calculations of potential energy surfaces. Single reference coupled cluster theory [12] and configuration interaction are two successful strategies capable of getting an accurate and reliable description of the correlation energy. As the result of the breakdown of single-reference theories in describing open-shell states, multi-reference theories are most desirable [13], where only one state at the time is to be conveniently considered [14, 15].

The formyl (HCO) radical is an important product formed from the interaction of Hydrogen and carbon monoxide, which has been the subject of extensive theoretical and experimental research for the past several decades (as surveyed by Marenich and Boggs [16]) but only a previous ab initio study was focused on the detailed calculation of the potential energy surface (PES) of the H···CO interaction in the vdW region [17]. In fact, detailed work by Lukeš et al. [17] at the UCCSD(T) level of theory, using a combination of POL1 atom-centered basis set [18] complemented with a set (3s,3p,2d) of optimized Tao's midbond functions [19, 20], revealed the presence of vdW minima in the PES of the ground state $H(^2S)\cdots CO(X^1\Sigma^+)$ complex at long interaction separations.

In the present study, we shall be concerned with the ground $H(^2S)\cdots CO(X^1\Sigma^+)$ and the excited $H(^2S)\cdots CO(a^3\Pi)$ electronic states of the H···CO complex interaction in the vdW region. The electronic structure of the low-lying states of HCO can be better understood starting from these two vdW structures [21]. The PES of these vdW complexes has predominant single-reference character, which allows us to use open-shell coupled cluster theories from a high-spin RHF reference wave function [22, 23]. This ansatz represents an alternative size-consistent economical method available for a reliable calculation of interaction energies. It will be also important to offer an educated guess of the electronic "vertical" excitation energies lying in the ultraviolet region, which can serve both as guideline for designing high resolution fluorescence spectra experiments to search for such system and, eventually, for the interpretation of the experimental results.

2 Methodology

The interaction potential of the H···CO vdW systems examined here has been obtained in the framework of the supermolecule approach at the partially spin restricted open-shell coupled cluster with perturbative triples corrections RHF-RCCSD(T) level of approximation for the total energy, as described by Knowles et al. [22, 23] and implemented in the MOLPRO package of ab initio programs [24]. In the present study, we have used the large *spdfg*-type basis set of Jankowski and Szalewicz [25], which includes a set of optimized bond function: 3s ($\alpha = 0.553063$, 0.250866, 0.117111), 2p ($\alpha = 0.392$, 0.142), 1d ($\alpha = 0.328$), to insure the best possible representation of the vdW dispersion interaction. The bond functions were placed at the midpoint of the vector **R**, which joins the center of mass of CO and H. This combination of atom-centered and midbond functions has been used successfully in describing the H_2···CO ground state interaction energy [25], keeping the size of the basis sets within practical limits with respect to resources as storage and computational time.

The interaction energy is defined as:

$$IE(\mathbf{R}) = E(H\cdots CO;\mathbf{R}) - E(H\cdots X;\mathbf{R}) - E(X\cdots CO;\mathbf{R}), \quad (1)$$

where E(H–X; **R**) and E(X–CO; **R**) are used here to indicate that the monomer energy (H and CO) is derived in the dimer-centered basis set. This amounts to apply the counterpoise procedure of Boys and Bernardi [26] to correct for the basis set superposition error at each molecular configuration **R**.

In contrast to closed-shell procedures, the counterpoise open-shell calculations cause additional complications for Π states. For example, the electron configuration of CO in its electronic excited $^3\Pi$ state corresponds to: $(1\sigma)^2$ $(1\sigma^*)^2(2\sigma)^2$ $(2\sigma^*)^2$ $(1\pi)^4$ $(3\sigma)^1$ $(2\pi^*)^1$. The degeneracy of the $2\pi^*$ orbital is removed by its partner H for any non-linear geometry of the molecular vdW complex. This Renner–Teller effect, lifts the degeneracy of these two states giving rise to the A′ and A″ (in Cs symmetry) states, respectively [27]. The A′ state corresponds to a configuration where the electrons occupy a π^* orbital located "parallel" to the C–O–H plane. In the A″ state, the electrons are occupying a π^* orbital located "perpendicular" to the C–O–H plane. All the calculations reported in the present contribution are based on the Bohr–Oppenheimer approximation, which provide A′ and A″ adiabatic potential-energy surfaces in the absence of spin-orbit splitting.

3 Results and discussion

3.1 Ground $H(^2S)\cdots CO(X^1\Sigma^+)$ state

In the present study, we have re-examined the H···CO ground-state energy as described in previous section, where all necessary energies were calculated by allowing all electrons to correlate. The final counterpoise-corrected interaction energies were computed according to Eq. 1, where the bond length of $CO(X^1\Sigma^+)$ was kept rigid at its experimental equilibrium bond length r(CO) of $2.1319a_o$ [28]. The H···CO geometry is specified by R, which

represents the distance between the center of mass of CO and H, and by the polar angle of orientation β of the vector along the C–O bond (directed from the C to the O atom), with respect to the vector along R. In this convention, $\beta = 0^\circ$ denotes the linear orientation H···C–O, while $\beta = 180^\circ$ designates the linear orientation H···O–C. Approaching $H(^2S)$ along a linear patch to $CO(X^1\Sigma^+)$ results in the ground $^2\Sigma^+$ state of the linear complex, which correlates to the X^2A' state along the bending coordinates.

The investigation of the PES was carried out for R ranging from 5 to $20a_o$ and for β every 11.25°, from 0° to 180°. The calculated grid of 334 counterpoise-corrected IE points were fitted to a function of the form

$$\mathrm{IE} = \sum_{i=0}^{10} \cos(\beta)^i \cdot \sum_{j=0}^{10} C_j \ \mathrm{Exp}\left[-b(R-a)\right]^j, \qquad (2)$$

where the energies are given in cm^{-1}. The least-square fitting parameters were obtained using *Matematica* [29] with a RMS error of 0.014 cm^{-1} and can be obtained from authors by request. The resulting contour plot of the PES for the X^2A' state with respect to R and β is depicted in Fig. 1, where points above 120 cm^{-1} were excluded from the fitting. The calculated IE reveals that the most stable configuration occurs at $\beta_e = 72^\circ$ with an equilibrium distance of $R_e = 6.89a_o$.

A plot of the maximum IE depth (with respect to R) along the angle β is depicted Fig. 2, which shows more clearly the equilibrium dissociation energy $D_e = 34.10$ cm^{-1} at $\beta_e = 72^\circ$ along the bending coordinate. The above figures

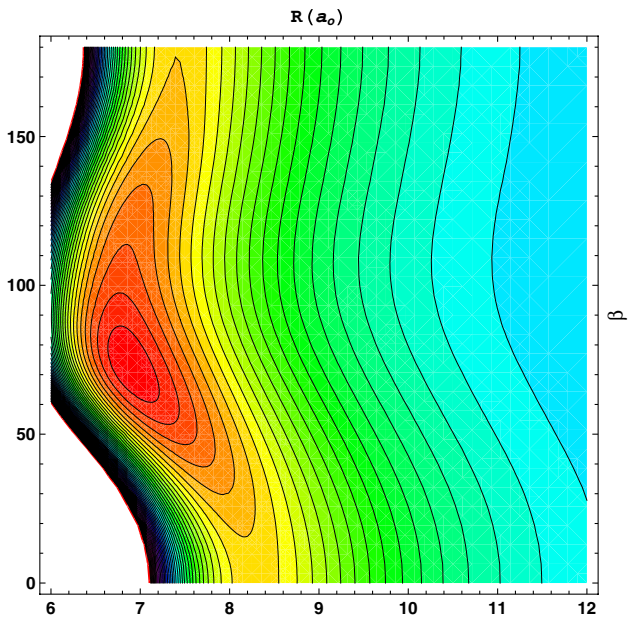

Fig. 1 Contour plot for the ground X^2A' state as a function of R and β at the RHF-RCCSD(T) level of theory. The *spacing* between the *lines* corresponds to 1.5 cm^{-1}

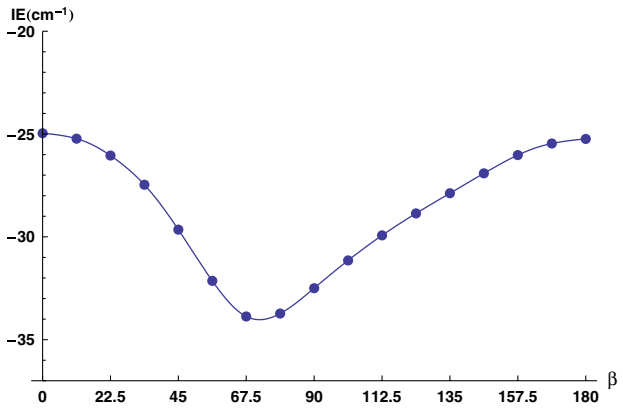

Fig. 2 Bending potential curve for the ground X^2A' state at the RHF-RCCSD(T) level of theory. The *values* represent the maximum IE depth with respect to R at each angle β. All energies are in cm^{-1}

also show that the linear orientations correspond to saddle points, with IE of -24.96 cm^{-1} at a distance of $R = 8.26a_o$ for $\beta = 0^\circ$ and IE of -25.49 cm^{-1} at a distance of $R = 7.41a_o$ for $\beta = 180^\circ$, which results in an forward activation energy of about 8.61 cm^{-1} (and of 9.14 cm^{-1} for the backward activation energy) along the bending coordinate. Further point wise optimization of the CO bond length of the $H(^2S)\cdots CO(X^1\Sigma^+)$ vdW complex at its equilibrium conformation ($\beta_e = 72^\circ$ and $R_e = 6.89a_o$) results in a value of r(CO) of $2.1379a_o$, which is $0.0060a_o$ longer than the original value of $2.1319a_o$ and makes the complex only 0.07 cm^{-1} more stable. Molecular orbital analysis reveals a weak bonding interaction among the **CO**(3σ) and **H**(1s) orbitals, which causes a bond weakening and further small increase in the bond distance of CO in the complex.

The present results are in close agreement with the values of $D_e = 34.35$ cm^{-1}, $\beta_e = 76^\circ$ and $R_e = 6.82a_o$ as found at the UCCSD(T) level of theory by Lukeš et al. [17], by using a slightly smaller CO bond length ($2.1316a_o$) and also a relative smaller basis set (POL1 + Tao). This comparison shows that, although the angular position of the minimum is changed by as much as 4°, the values of R_e and D_e are only marginally affected by the change to a more accurate basis set. It would be of great interest at this point to investigate, by using intermolecular perturbation theory, how the physical origin of the present PES anisotropy compares to previous results [17].

3.2 Excited $H(^2S)\cdots CO(a^3\Pi)$ state

Although the $CO(X^1\Sigma^+) \rightarrow CO(a^3\Pi)$ transition is well known experimentally [30], there is no any direct experimental evidence of the formation of the excited $H(^2S)\cdots CO(a^3\Pi)$ complex. Since we are interested in vertical excitation energies, the supermolecule IE calculations were performed at different geometries (as specified

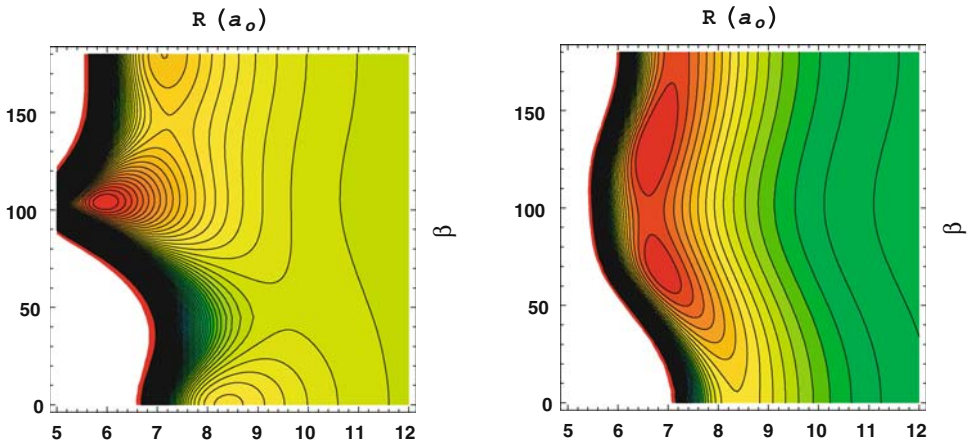

Fig. 3 Contour plots for the excited states $^4A'$ (in *panel a*) and $^4A''$ (in *panel b*) as a function of R and β at the RHF-RCCSD(T) level of theory. The *spacing* between the *lines* corresponds to 3.2 cm^{-1} for $^4A'$ and 2.2 cm^{-1} for $^4A''$

by R and by the Jacobi angle of orientation β) but keeping the stretching coordinates of CO fixed at the ground bond length of $2.1319a_o$. As for the ground state, the necessary energies were calculated allowing all the electrons to correlate. Approaching $H(^2S)$ along a linear patch to $CO(a^3\Pi)$ leads to the excited $^4\Pi$ state of the linear vdW complex. As explain before, the Renner–Teller effect will split the linear $^4\Pi$ state into the $^4A'$ and $^4A''$ states along the bending coordinate. As before, the calculated PES was obtained for R ranging from 5 to $20a_o$ and for β ranging from 0° to 180°. The calculated grid of counterpoise-corrected IE points was fitted to a function of the form given by Eq. 2 by using *Matematica* [29].

The resulting IE contour plots of the excited $^4A'$ and $^4A''$ states are depicted in Fig. 3a and b, respectively, where points above 120 cm^{-1} were excluded from the fitting. In order to account for the larger anisotropy of the resulting PESs, the grid was increased, as compared to the ground state, to 717 and 528 points, which allows to obtain a final small RMS error in the fitting of 0.010 and 0.012 cm^{-1}, respectively (fitting parameters can be obtained from authors by request). The corresponding plots of the maximum depth of IE (with respect to R) along the bending coordinate (defined by the angle β) for the $^4A'$ and $^4A''$ states are depicted in Fig. 4.

The resulting IE of the excited $^4A''$ state reveals two minima separated by a saddle point. The most stable configuration occurs at $\beta_e = 132°$ and $R_e = 6.71a_o$ with an equilibrium dissociation energy of $D_e = 40.03$ cm^{-1}. The second minimum occurs at $\beta = 68°$ and $R = 6.90a_o$ with a depth of 38.31 cm^{-1}. The saddle point connecting these minima is located at $\beta = 96°$ and $R = 6.64a_o$ with a depth of 36.12 cm^{-1}. This results in a forward energy barrier of 2.69 cm^{-1} in going from the minimum at $\beta = 68°$ to the minimum at $\beta = 96°$ (and of 3.89 cm^{-1} for the backward energy barrier) along the reaction coordinate. Point wise optimization of the CO bond length in the $^4A''$ state of the $H(^2S)\cdots CO(a^3\Pi)$ complex at its equilibrium conformation

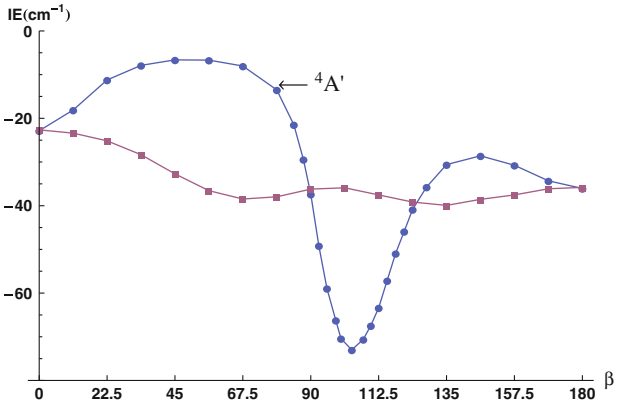

Fig. 4 Bending potential curves at the RHF-RCCSD(T) level of theory for the $^4A'$ and $^4A''$ excited states. The *values* represent the maximum IE depth with respect to R at each angle β. All energies are in cm^{-1}

($\beta_e = 132°$ and $R_e = 6.71a_o$) results in a value of $2.2816a_o$, which makes the complex 2.07 cm^{-1} more stable than its unrelaxed counterpart does. In the $^4A''$ state, the $CO(2\pi^*)$ antibonding orbital is "perpendicular" to the C–O–H plane, which does not have the right symmetry to bond with the H(1s) orbital. Thus, it is again the weak bonding interaction among the $CO(3\sigma)$ and H(1s) orbitals (although relative stronger than in the ground state) that causes the bond weakening and further increase in the bond CO distance in the complex.

The calculated PES for the excited $^4A'$ state reveals that the most stable configuration occurs at $\beta_e = 104°$ at an equilibrium distance of $R_e = 5.90a_o$ with an equilibrium dissociation energy of $D_e = 75.42$ cm^{-1}. It also reveals two saddle points with IE of -6.56 cm^{-1} at a distance of $R = 9.58a_o$ for $\beta = 51°$ and IE of -28.56 cm^{-1} at a distance of $R = 7.22a_o$ for $\beta = 145°$, which connect the absolute minimum with secondary minima located at $\beta = 0°$ and $\beta = 180°$, respectively. This result in forward activation energy of 46.86 cm^{-1}, and of 68.86 cm^{-1} for

the backward activation energy along the reaction coordinate. Further point wise optimization of the CO bond length of the $^4A'$ state of the $H(^2S)\cdots CO(a^3\Pi)$ complex at its equilibrium conformation ($\beta_e = 104°$ and $R_e = 5.90a_o$) results in a value of $1.7501a_o$, which makes the complex a significant 18.88 cm^{-1} more stable than its un-relaxed counterpart does. In view of the relative large geometry relaxation experimented by point-wise optimization of the CO bond length in the $^4A'$ state of the $H(^2S)\cdots CO(a^3\Pi)$ complex frozen at its equilibrium conformation, we leave open the possibility of optimizing simultaneously r(CO), R and β in order to find a more accurate minimum for this electronic state. In this state, the CO(2π*) orbital is located "parallel" to the C–O–H plane and it has the right symmetry to form a relative strong bonding interaction with the H(1s) orbital, which in turn, withdraws electron density from the antibonding CO(2π*) orbital to stabilize it and further decrease the bond CO distance in the complex.

3.3 DFT representation of the ground state

In view of the recent successfully reported study on the structure and bonding properties of the ground $N_2(X^1\Sigma_g^+)\cdots He(^2S)$ electronic state by means of the mPW1PW exchange–correlation functional of Adamo and Barone [31], using DFT local-spin-optimized atom-centered basis sets complemented with bond functions optimized at the mPW1PW level of theory [32], we have decided to perform similar less-demanding calculations on the ground $H(^2S)\cdots CO(X^1\Sigma^+)$ electronic states of H···CO, which are to be compared to the RHF-RCCSD(T) reference calculations presented in Sect. 3.1. The DFT calculations were performed in the framework of the supermolecule approach applying the Kohn–Sham formalism [33], where the counterpoise-corrected interaction energy is defined as before by Eq. 1. The mPW1PW [31] exchange–correlation functional was tested as implemented in the Gaussian 03 molecular package [34] for the total energy. In the DFT calculations, we have used the TZVP atom-centered Gaussian basis sets, which have been optimized for local-spin DFT calculations by Godbout et al. [35]. They were complemented with a basis set of bond functions modified to increase the ground-state dispersion-energy interaction at the mPW1PW level of theory. These DFT-optimized bond functions are referred here as BF-DFT, and they consist of three s functions (exponents 1.1, 0.3 and 0.1), two p functions (exponents: 0.9, 0.3), one d functions (exponents: 0.6), one f function (exponent: 0.5) and one g function (exponent: 0.5) placed at the midpoint of the vector **R** joining the center of mass of CO and H, where the bond length of $CO(X^1\Sigma^+)$ was kept rigid at its experimental equilibrium bond length r(CO) of $2.1319a_o$.

The resulting PES of the ground $H(^2S)\cdots CO(X^1\Sigma^+)$ electronic states of H···CO at the mPW1PW/TZVP + BF − DFT level of theory reveals a single-minimum surface with the most stable configuration located at $\beta_e = 79°$, $R_e = 8.46a_o$ and dissociation energy $D_e = 11.21$ cm^{-1}, which is too shallow as compare to the reference calculation ($D_e = 34.10$ cm^{-1} at $\beta_e = 72°$). This can be seen clearly from the plot of the maximum depth of IE (with respect to R) along the angle β as depicted in Fig. 5, where the ground RHF-RCCSD(T) reference calculation (lower curve) is also included for comparison. This figure shows that the linear orientations correspond to the saddle points, with IE of -3.09 cm^{-1} for $\beta = 0°$ and IE of -3.48 cm^{-1} for $\beta = 180°$, which results in an forward activation energy of 7.72 cm^{-1} and of 9.11 cm^{-1} for the backward activation energy along the reaction coordinate. These values compare relative well to the values of 8.61 cm^{-1} and of 9.14 cm^{-1} obtained for the reference calculations. Further point wise optimization of the CO bond length of the complex $H(^2S)\cdots CO(X^1\Sigma^+)$ at its equilibrium conformation ($\beta_e = 79°$ and $R_e = 8.46a_o$) results in a value of r(CO) of $2.1371a_o$, which is $0.0052a_o$ longer than the the original value of $2.1319a_o$ (making the complex only 0.02 cm^{-1} more stable) in complete agreement also with the reference results for thr r(CO) optimization presented in Sect. 3.1.

Although the PES is too shallow as compare to the reference RHF-RCCSD(T) calculations, Fig. 5 shows that, on the whole, the exchange–correlation functional mPW1PW [31] using DFT-optimized bond functions [32] gives an "excellent" qualitative representation of the interaction energy of the ground $H(^2S)\cdots CO(X^1\Sigma^+)$ electronic states of vdW H···CO complex, where the detailed anisotropy of the potential is undoubtedly very well represented. Since the mPW1PW/TZVP + BF − DFT potential resulted too

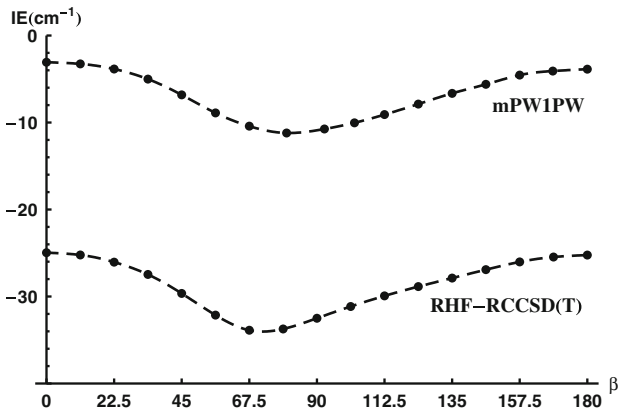

Fig. 5 Bending potential curve for the ground X^2A' state at the mPW1PW and RHF-RCCSD(T) levels of theory. The *values* represent the maximum IE depth with respect to R at each angle β. All energies are in cm^{-1}

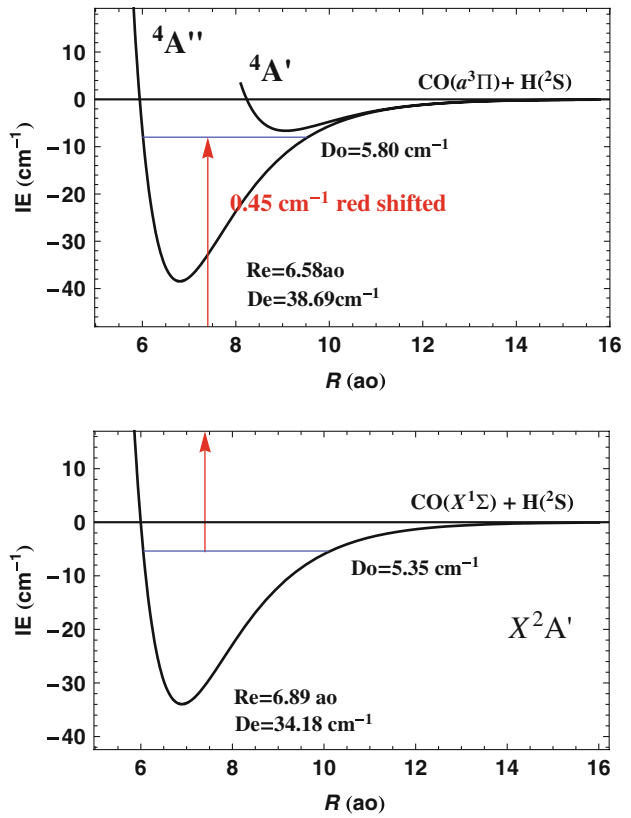

Fig. 6 Vertical $X^2A' \rightarrow {}^4A'$ excitation for H···CO at its "tilted" most-stable ground X^2A' state geometry [r(CO) = 2.1379a_o and $\beta = 72°$]

shallow for the ground state (although qualitatively correct), no further steps were taken to ansatz for the excited states.

3.4 Excitation energy

In this section, we present the electronic "vertical" excitation energies for the H···CO vdW complex using a one-dimensional stretching model, which can be used to set up initial experimental conditions in laser induced fluorescence spectroscopy experiments of H gas seeded with CO at low temperatures. This simple stretching model has been presented previously by Salazar et al. for He···CO [36], and more recently for He···CO$^+$ [37] and Ar···CO [38]. The $H(^2S)\cdots CO(X^1\Sigma^+) \rightarrow H(^2S)\cdots CO(a^3\Pi)$ vertical excitation spectrum of H···CO, frozen at its "tilted" most-stable ground-state geometry [r(CO) = 2.1379a_o and $\beta = 72°$] is depicted in Fig. 6. The calculated counterpoise-corrected IE points were fitted to a function of the form given in Eq. 2, but only in the stretching coordinate R. The least-square fitting parameters were again obtained using *Mathematica* [23] with a RMS error of 0.008 cm^{-1}. Vibrational energies were calculated from the fitted potential curves using the numerical Numerov–Cooley procedure [39] by treating H–CO as a diatomic system with only one degree of freedom R. This procedure shows that for the ground X^2A' electronic state (lower curve in Fig. 6), the minimum occurs at R_e of 6.89a_o, D_e = 34.18 cm^{-1} and the calculated dissociation energy corresponds to D_o = 5.35 cm^{-1}, with only one vibrational states supported by this ground IE curve. Present calculations also shows that the minimum of the excited $^4A''$ interaction (upper curve in Fig. 6), occurs at R_e of 6.58a_o, D_e = 38.69 cm^{-1} and D_o = 5.80 cm^{-1}, with only one vibrational states supported by this excited state. This amounts to a small red shift of 0.45 cm^{-1} for the transition $X^2A' \rightarrow {}^4A'$ with respect to the corresponding $CO(X^1\Sigma^+) \rightarrow CO(a^3\Pi)$ excitation in absence of H. In addition, the upper panel of Fig. 6 depicts the fitted potential of the excited $^4A'$ state with R_e of 8.60a_o and D_e = 9.63 cm^{-1}, which does not support any vibrational state.

After vertical excitation from the ground state, the excited $CO(a^3\Pi)\cdots H(^1S)$ state could relax its geometry before the optical transition back to the ground state. In particular, it is noticeable from Fig. 4 the relative large geometry relaxation experimented by the excited $^4A'$ state, which is thus studied in more detail here. The vertical $^4A' \rightarrow X^2A'$ emission is depicted in Fig. 7, where the conformation of the ground X^2A'state is frozen at the most stable excited $^4A'$ geometry [r(CO) = 1.7502a_o and $\beta = 104°$]. Vibrational energies were calculated from the fitted potential curves (as explained above) by using again the numerical Numerov-Cooley procedure [39]. This procedure shows that for the excited $^4A'$ electronic state (upper curve in Fig. 7), the optimal calculated interaction occurs at R_e of 5.73a_o, D_e = 92.32 cm^{-1} and the dissociation energy corresponds to D_o = 30.88 cm^{-1}, with only one vibrational state supported by this excited IE curve. Present calculations also show that the minimum of the ground X^2A' interactions (lower curve in Fig. 7) occurs at R_e of 6.78a_o, D_e = 27.95 cm^{-1} and D_o = 2.56 cm^{-1}, with only one vibrational state supported. We can see that after relaxation, vertical emission shows a large red shifts of 28.32 cm^{-1} for the $^4A' \rightarrow X^2A'$ transition, with respect to the corresponding $CO(a^3\Pi) \rightarrow CO(X^1\Sigma^+)$ transition in absence of H.

4 Final remarks

In the present study, ab initio calculations at the RHF-RCCSD(T) level of theory in the framework of the supermolecule approach were used to study the H···CO vdW complex. The interaction energy of the ground $H(^2S)\cdots CO(X^1\Sigma^+)$ and excited $H(^2S)\cdots CO(a^3\Pi)$ electronic states, as a function of the distance R between the H atom and the center of mass of CO and the angle β among the monomers, were determined in order to calculate the

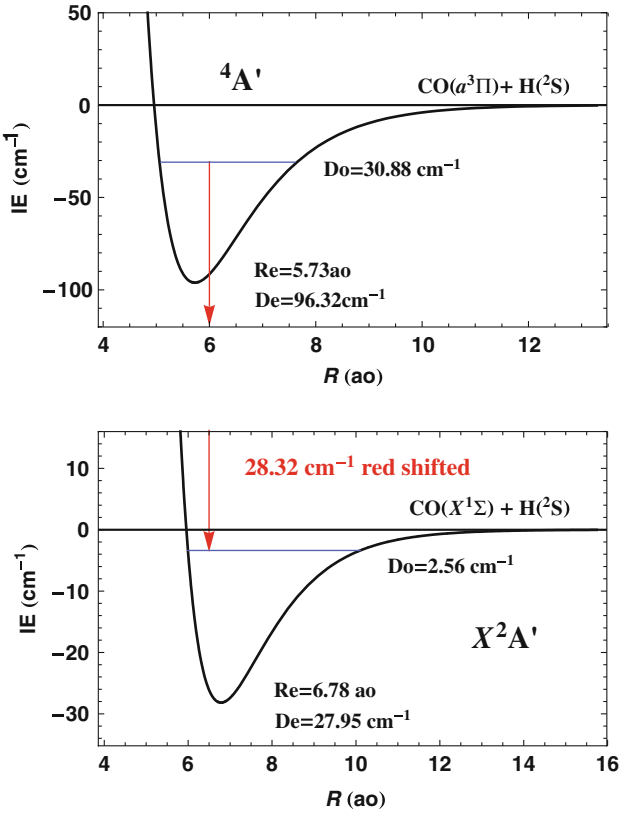

Fig. 7 Vertical $^4A' \rightarrow X^2A'$ transition for H···CO at its "tilted" most-stable excited $^4A'$ state geometry [$r(CO) = 1.7502a_o$ and $\beta = 104°$]

corresponding equilibrium values: β_e, R_e and D_e. These calculations indicated a ground X^2A' most-stable interaction with $\beta_e = 72°$, $R_e = 6.89a_o$ and $D_e = 34.10\ cm^{-1}$ and an excited most-stable $^4A'$ interaction with $\beta_e = 104°$, $R_e = 5.90a_o$ and $D_e = 75.42\ cm^{-1}$. They also indicate and excited $^4A''$ state with two minima separated by a saddle point: the most stable configuration occurring at $\beta_e = 132°$, $R_e = 6.71a_o$ and $D_e = 40.03\ cm^{-1}$ with the secondary minimum occurring at $\beta_e = 68°$, $R_e = 6.90a_o$ and $D_e = 38.31\ cm^{-1}$.

Calculations at the mPW1PW/TZVP + BF − DFT level of theory for the ground $H(^2S)\cdots CO(X^1\Sigma^+)$ electronic state of the vdW H···CO complex revealed that the resulting PES is too shallow as compare to the reference RHF-RCCSD(T) calculations. Nevertheless, it gives an "excellent" qualitative representation of the interaction energy, where the detailed anisotropy of the potential is undoubtedly very well represented. In our opinion, density functional theory calculations with the mPW1PW exchange–correlation functional using DFT local-spin-optimized atom-centered basis sets complemented with DFT-optimized bond functions are qualitatively correct and can be used as a guideline for more demanding computational work on ground-state vdW complexes.

A small red shifts of $0.45\ cm^{-1}$ was obtained for the $X^2A' \rightarrow {}^4A''$ vertical excitation energy with respect to the corresponding $CO(X^1\Sigma^+) \rightarrow CO(a^3\Pi)$ excitation in absence of H, while the electronic $^4A'$ state remains inaccessible by a vertical excitation from the ground X^2A' electronic state frozen at its "tilted" most-stable ground-state geometry: $r(CO) = 2.1379a_o$ and $\beta = 72°$. A relaxed vertical $^4A' \rightarrow X^2A'$ transition is also described (where the conformations of the electronic states involved are frozen at the most-stable $^4A'$ state geometry: $r(CO) = 1.7502a_o$ and $\beta = 104°$), which exhibits a large red shifts of $28.32\ cm^{-1}$ with respect to the corresponding $CO(a^3\Pi) \rightarrow CO(X^1\Sigma^+)$ transition in absence of H. All the vertical excitation spectra described here are to be taken as a qualitative guide because we have only included the most stable conformer into account. A realistic approach must involve the complete IE surfaces for both the ground and excited states, which is underway in our laboratory and the results will be published elsewhere.

Acknowledgments The authors thank, the Fondo Nacional De Ciencia, Tecnologia e Innovacion FONACIT (Grants: G-97000741 and G-97000593) and to the "Decanato De Investigaciones" of the Simón Bolívar University (Grant GID-13) for continuous support of the present research work.

References

1. Hobza P, Zahradník R (1988) The role of van der Waals systems in physical chemistry and in biodisciplines, studies in physical and theoretical chemistry, vol 52. Elsevier, Amsterdam, p 13
2. Hobza P, Zahradnik R (1980) Weak intermolecular interaction in chemistry and biology. Elsevier, Amsterdam, p 201
3. Tielen AGGM (1992) In: Saito D (ed) Chemistry and spectroscopy of interstellar molecules. University of Tokyo Press, Tokyo, p 237
4. McKellar ARW (1982) Faraday Discuss Chem Soc 73:89. doi: 10.1039/dc9827300089
5. McKellar ARW (1990) J Chem Phys 93:18. doi: 10.1063/1.459591
6. Chan M-C, McKellar ARW (1996) J Chem Phys 105:7910
7. Chuaqui CE, Le Roy RJ, McKellar ARW (1994) J Chem Phys 101:39
8. Jäer W, Gerry MCL (1992) Chem Phys Lett 196:274. doi: 10.1016/0009-2614(92)85967-F
9. Xu Y, McKellar ARW (1996) Mol Phys 88:859. doi: 10.1080/00268979650026343
10. Maitland GC, Rigby M, Smith EB, Wakeham WA (1981) Intermolecular forces their origin and determination. Oxford University Press, Oxford
11. Dykstra CE, Liu S-Y (1987) In: Weber A (ed) Structure and dynamics of weakly bound molecular complexes. Reidel, Dordrecht, pp 2069
12. Bartlett RJ (1995) In: Yarkony DR (ed) Modern electronic structure theory. World Scientific, Singapore
13. Buenker RJ, Krebs S (1999) In: Hirao K (ed) Recent advances in Multireference Methods. World Scientific, Singapore 131:160
14. Malrieu JP, Durand P, Daudey JP (1985) J Phys Math Gen 18:809. doi:10.1088/0305-4470/18/5/014

15. Mahapatra US, Datta B, Bandyopadhyay B, Mukherjee D (1998) Adv Quantum Chem 30:163. doi:10.1016/S0065-3276(08)60507-9
16. Marenich AV, Boggs JE (2003) J Phys Chem 107:2343
17. Lukeš V, Laurinc V, Ilcin M, Biskupic S (2004) Collect Czech Chem Commun 69:1. doi:10.1135/cccc20040001
18. Sadlej AJ (1998) Collect Czech Chem Commun 53:1995
19. Tao F-M, PanY-K (1992) J Chem Phys 97:4989
20. Tao F-M (1992) J Chem Phys 98:3049. doi:10.1063/1.464131
21. Serrano-Andrés L, Forsberg N, Malmqvist P (1998) J Chem Phys 108:7202. doi:10.1063/1.476138
22. Knowles PJ, Hampel C, Werner H-J (1993) J Chem Phys 99:5219
23. Knowles PJ, Hampel C, Werner H-J (2000) J Chem Phys 112:3106. doi:10.1063/1.480886
24. Werner H-J, Knowles PJ, Lindh R, Schütz M et al (2006) MOLPRO, version 2006.1, a package of ab initio programs
25. Jankowski P, Szalewicz K (1998) J Chem Phys 106:3554. doi:10.1063/1.475347
26. Boys S, Bernardi F (1970) Mol Phys 19:553. doi:10.1080/00268977000101561
27. Wagne F, Dunning T, Kok R (1994) J Chem Phys 100:1326. doi:10.1063/1.466610
28. Herzberg G (1950) Molecular spectra and molecular structure I. Spectra of diatomic molecules. Van Nostrand Reinhold, New York
29. Wolfram Research Inc (2007) Mathematica, Version 6.0.0, Champaign, IL
30. Huber KP, Herzberg G (1979) Constants of diatomic molecules. van Nostrand, New York
31. Adamo C, Barone V (1998) J Chem Phys 108:664. doi:10.1063/1.475428
32. Salazar MC, Paz JL, Hernández AJ, Manzanares C, Ludeña E (2001) Theor Chem Acc 106:218. doi:10.1007/s002140100251
33. Kohn W (1999) Rev Mod Phys 71:1253. doi:10.1103/RevModPhys.71.1253
34. Frisch MJ, Trucks GW, Schlegel HB, Scuseria GE, Robb MA, Cheeseman JR, Montgomery Jr JA, Vreven T, Kudin KN, Burant JC, Millam JM, Iyengar SS, Tomasi J, Barone V, Mennucci B, Cossi M, Scalmani G, Rega N, Petersson GA, Nakatsuji H, Hada M, Ehara M, Toyota K, Fukuda R, Hasegawa J, Ishida M, Nakajima T, Honda Y, Kitao O, Nakai H, Klene M, Li X, Knox JE, Hratchian HP, Cross JB, Bakken V, Adamo C, Jaramillo J, Gomperts R, Stratmann RE, Yazyev O, Austin AJ, Cammi R, Pomelli C, Ochterski JW, Ayala PY, Morokuma K, Voth GA, Salvador P, Dannenberg JJ, Zakrzewski VG, Dapprich S, Daniels AD, Strain MC, Farkas O, Malick DK, Rabuck AD, Raghavachari K, Foresman JB, Ortiz JV, Cui Q, Baboul AG, Clifford S, Cioslowski J, Stefanov BB, Liu G, Liashenko A, Piskorz P, Komaromi I, Martin RL, Fox DJ, Keith T, Al-Laham MA, Peng CY, Nanayakkara A, Challacombe M, Gill PMW, Johnson B, Chen W, Wong MW, Gonzalez C, Pople JA (2004) Gaussian 03, Revision C.02, Gaussian Inc, Wallingford CT
35. Godbout N, Salahub DR, Andzelm J, Wimmer E (1992) Can JChem 70:560. doi:10.1139/v92-079
36. Salazar MC, Paz JL, Hernández AJ, Castejón HJ (2001) J Mol Struct Theochem 539:119. doi:10.1016/S0166-1280(00)00779-X
37. Salazar MC, Lugo I, Hernández AJ, Manzanares C (2005) Theor Chem Acc 115:246. doi:10.1007/s00214-005-0009-9
38. Castejon H, Salazar MC, Paz JL, Hernandez AJ (2006) J Mol Struct Theochem 801:1. doi:10.1016/j.theochem.2006.08.021
39. Davie K, Wallace R (1988) Comput Phys Commun 51:217. doi:10.1016/0010-4655(88)90073-2